In vitro Study of Root Fracture Treated by CO₂ Laser and DP-bioactive Glass Paste

Yin-Lin Wang,[1] Bor-Shiunn Lee,[1] Ching-Li Tseng,[2] Feng-Huei Lin,[2] Chun-Pin Lin[1]*

Background/Purpose: An ideal material has yet to be discovered that can successfully treat vertical root fracture. Therefore, the purpose of this study was to use a continuous-wave CO_2 laser of medium-energy density to fuse DP-bioactive glass paste (DPGP) to vertical root fracture.

Methods: The DP-bioglass powder was based on a $Na_2O\text{-}CaO\text{-}SiO_2\text{-}P_2O_5$ system and it was mixed with phosphoric acid (65% concentration) with a powder/liquid ratio of 2 g/4 mL to form DPGP. The interaction of DPGP and dentin was analyzed by means of X-ray diffractometer (XRD) and differential thermal analysis/thermogravimetric analysis (DTA/TGA). Root fracture line was filled with DPGP followed by CO_2 laser irradiation and the result was examined by scanning electron microscopy (SEM).

Results: The main crystal phase of DPGP was monocalcium phosphate monohydrate ($Ca(H_2PO_4)_2 \cdot H_2O$) and the phase transformed to dicalcium phosphate dihydrate ($CaHPO_4 \cdot 2H_2O$) after mixing DPGP with dentin powder (DPG-D). Additionally, $\gamma\text{-}Ca_2P_2O_7$ and $\beta\text{-}Ca_2P_2O_7$ were identified when DPG-D was lased by CO_2 laser. The reaction temperature was between 500°C and 1100°C. SEM results demonstrated that the fracture line was effectively sealed by DPGP.

Conclusion: The chemical reaction of DPGP and dentin indicated that DPGP combined with CO_2 laser is a potential regimen for the treatment of vertical root fracture. [*J Formos Med Assoc* 2008;107(1):46–53]

Key Words: CO_2 laser, DP-bioactive glass paste, vertical root fracture

Vertical root fracture has long been a troublesome symptom that is difficult to diagnose accurately and to treat effectively. It can be caused by numerous factors including volumetric expansion of post-corrosion, pin and post placement, seating of intracoronal restorations, and spreader loads during lateral condensation of the gutta-percha.[1–4] The spreader loads required to cause vertical root fracture were demonstrated to be as small as 1.5 kg and 7.2 kg in human mandibular incisors and maxillary central incisor, respectively.[5,6]

The current concept of treating vertical root fracture is to fill the crack line with materials to avoid any communication between the periodontium and the main canal. These proposed materials included 4-META/MMA-TBB adhesive resin,[7] glass-ionomer bone cement,[8] mineral trioxide aggregate,[9] and cyanoacrylate.[10] However, these materials cannot strongly bond to dentin or they exhibit low biocompatibility. Consequently, in the majority of cases of vertical root fracture, the long-term prognosis is poor and tooth extraction is usually the final resolution.

[1]School of Dentistry and Graduate Institute of Clinical Dentistry, College of Medicine, National Taiwan University and National Taiwan University Hospital, and [2]Institute of Biomedical Engineering, College of Medicine, National Taiwan University, Taipei, Taiwan.

Correspondence to: Dr Chun-Pin Lin, School of Dentistry and Graduate Institute of Clinical Dentistry, College of Medicine, National Taiwan University, 1 Chang-Te Street, Taipei 100, Taiwan.
E-mail: pinlin@ntu.edu.tw

ELSEVIER

Since the debut of laser research in dental literature, numerous studies in the past 40 years have broadened the application of lasers in dentistry. One of the most used lasers in clinical treatment, the CO_2 laser, has been approved by the Food and Drug Administration (FDA) to be used in soft tissue management. Although the thermal effect induced by CO_2 laser limits its application in dental hard tissues, CO_2 laser can provide exceedingly rapid temperature elevation followed by fast cooling once the irradiation is ceased. Therefore, CO_2 laser was proposed to fuse the vertical root fracture.[11] However, the glaze layer produced by CO_2 laser irradiation could not provide a reliable bond against mastication and a hermetic seal could not be achieved for fractures with large gaps, indicating that an ideal treatment method for vertical root fracture is still needed to be developed.

Bioglass is a highly biocompatible material and has a high surface reactivity that can induce osteogenesis in physiologic systems.[12] We have demonstrated promising results from an *in vitro* study by using laser and bioglass for the treatment of dentin hypersensitivity.[13,14] As a paste with a low melting temperature and low viscosity in liquid state is optimal for the fusion of vertical root fracture, DP-bioactive glass with a low melting temperature was mixed with phosphoric acid to form DP-bioactive glass paste which could adhere to tooth structures. In addition, the spectral output of the CO_2 laser is about 940–1060 nm, which overlaps with the strong absorption ranges of dental apatite and DP-bioglass.[15–17] Therefore, CO_2 laser was employed to help the fusion of DP-bioactive glass paste to the fracture line.

The aim of this study was to use a continuous-wave CO_2 laser to fuse DP-bioactive glass paste to vertical root fracture and to bridge the fracture line. The thermal interactions and bridging mechanism between DP-bioactive glass paste and dentin when subjected to CO_2 laser were studied by X-ray diffractometer (XRD), differential thermal analysis (DTA)/thermogravimetric analysis (TGA), and scanning electron microscopy (SEM).

Methods

Preparation of the glass paste

Powder mixtures of various normal compositions in the glass-forming region of Na_2O-CaO-SiO_2-P_2O_5 were prepared by using reagent-grade chemicals of Na_2CO_3, $CaCO_3$, SiO_2 and $Ca_3(PO_4)_2$ (Aldrich Co., Milwaukee, WI, USA). They were mixed in a ball mill pot and ethanol was added to wet-mill the powder together. The powder was dried overnight and placed in a platinum crucible. The crucible with the powder was placed in a SiC furnace and was heated to 1410°C for 1.5 hours. Thereafter, it was removed from the furnace and the melted glass was poured into water to quench. The glass was milled and sieved to 36 μm. The DP-bioglass powder so obtained was mixed with phosphoric acid (65% concentration) with a powder/liquid ratio of 2 g/4 mL to form a gel. The gel-like material was named DP-bioactive glass paste (DPGP).

Preparation of tooth specimen

Twenty extracted human incisors were used, with informed consent at the National Taiwan University Hospital, for this study. Crowns with caries, restorations, or fractures were discarded. Any remaining soft tissue was thoroughly removed from the tooth surface with a dental scaler (Sonicflex 2000, KaVo Co., Biberbach, Germany). All teeth were then stored in 4°C distilled water containing 0.2% thymol to inhibit microbial growth until use.

While hydrated, the root was cut at a site 1 mm below the cementoenamel junction, parallel to the direction of dentinal tubule and perpendicular to the long axis of the tooth, by means of a low-speed diamond wafering blade (Isomet; Buehler Ltd., Lake Bluff, IL, USA). A longitudinal groove with a dimension of 1×5 mm^2 and a depth of 1.5 mm was prepared by a high-speed fissure bur on either the labial or lingual surface of the root. Each specimen was immersed in 17% EDTA followed by 2 minutes of ultrasonic vibration to remove the smear layer, then rinsed with copious distilled water and dried with clean air. DPGP was then packed into the groove and the

specimen was subjected to the CO_2 laser treatment. To obtain a section containing dentin-DPGP interface, the root was sectioned 2 mm thick, perpendicular to the groove, by a low-speed diamond saw running under water. Specimens made by this method were prepared for SEM observation.

However, it was difficult to analyze the dentin-DPGP interface by XRD and thermal analysis. Some dentin blocks were pulverized into powder of an average particle size of 106 μm. The dentin powder was mixed with the DP-bioactive glass paste, with a mixing ratio of 1:1, to form a mixture named DPG-D. The mixture was then prepared for XRD and DTA/TGA analysis.

Laser parameters

The LUXAR LX-20 CO_2 laser (Luxar Corp., Bothell, WA, USA) was operated at the power setting of 5 W, using a focused (2 mm from target surface) continuous waveform beam delivered through a 0.8 mm diameter ceramic tip. The efficiency of the delivery of beam energy was 86% as determined by the manufacturer of the model. The time for each exposure was 5 seconds and the total irradiation time was 1 minute. Thus, the calculated energy density was 2500 J/cm². Before irradiation, powder form specimen was compacted into a disc (3 mm in diameter and 1 mm in thickness) with a hydraulic force of 50 kg/cm², to prevent the powder from rising up or fluttering in the air during laser beam sputtering.

XRD

The crystalline phases of the specimens before and after laser irradiation were determined by a Rigaku X-ray powder diffractometer (Rigaku Denki Co., Ltd., Tokyo, Japan) with CuKα radiation and Ni filter. The scanning range of 2θ was from 10 degrees to 60 degrees with a scanning speed of 4 degrees/min. To determine the contents of different phases, relative intensities of the characteristic peaks of each phase were used.

DTA/TGA

The thermal behaviors before and after laser irradiation were recorded by a TA/SDT2960 (Thermal Analysis Instruments Inc., New Castle, DE, USA) for DTA and TGA. The scanning temperature was from room temperature up to 1500°C, with a heating rate of 20°C/min and N_2 flow rate of 90 mL/min. The total weight of the specimen for each thermal analysis was 20 mg, using Al_2O_3 as the reference powder.

SEM

The morphology and microstructure of the specimens before and after laser treatment were observed under SEM. The specimens were immersed in 2.5% cold glutaraldehyde in 0.1 mol/L cacodylate buffer at pH 7.4 for 8 hours. Subsequent to initial fixation, the specimens were rinsed in buffer and post-fixed with 1% osmium tetraoxide for 4 hours. All specimens were then serially dehydrated in graded ethanol solutions (50, 60, 70, 80, 90, 95, 100% ethanol) at 45-minute intervals, and the critical point dried. Finally, all specimens were mounted on aluminum stubs and sputter-coated with ~200 Å gold before being examined under a Hitachi SEM (Model S-800, Tokyo, Japan).
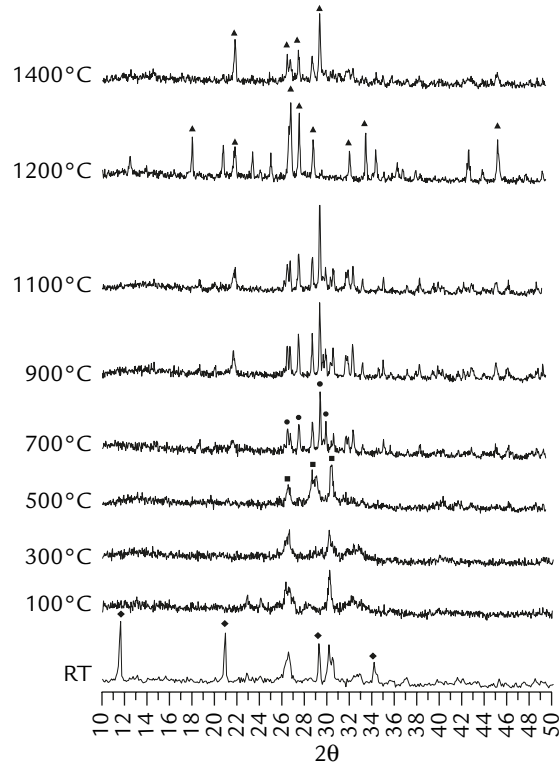
Results

XRD analysis

Figure 1 shows the X-ray diffraction pattern of DPGP, dentin powder, DPGP mixed with dentin powder (DPG-D), and DPG-D after CO_2 laser irradiation, respectively. The DPGP prepared by mixing the glass with 65% phosphoric acid demonstrated a pattern with two crystalline phases, which were identified as monocalcium phosphate monohydrate $(Ca(H_2PO_4)_2 \cdot H_2O)$ and silicate pyrophosphate (SiP_2O_7) from the standard Joint Committee on Powder Diffraction Standards (JCPD) card. The X-ray diffraction pattern of dentin powder, shown in Figure 1B, represented a non-stoichiometric hydroxyapatite crystalline phase. The characteristic peaks of dentin were broad and fairly weak, which indicated that the dentin was not well-crystallized due to its smaller particle size. Figure 1C shows that after mixing the DPGP with
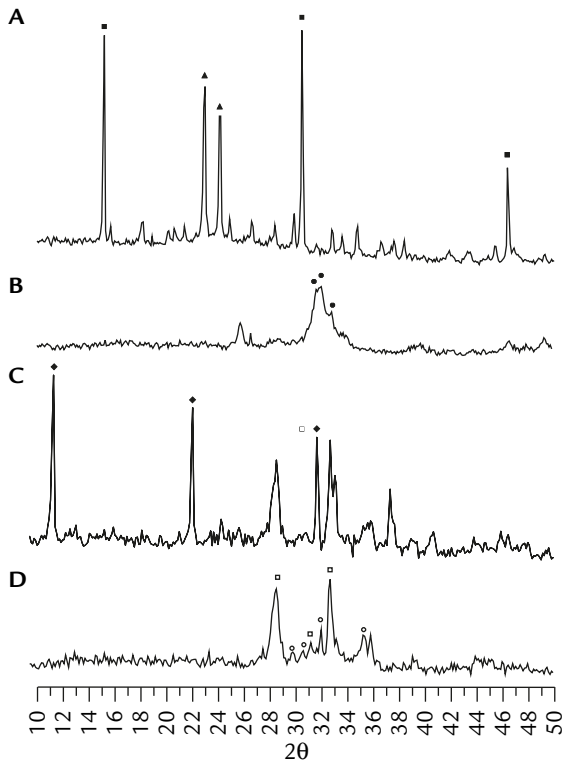
Figure 1. X-ray diffraction patterns of: (A) DP-bioactive glass paste (DPGP); (B) dentin powder; (C) mixture (DPG-D) of DPGP and dentin powder; and (D) DPG-D after CO$_2$ laser treatment. ▲ = Ca(H$_2$PO$_4$)$_2$·H$_2$O; ■ = Si$_2$P$_2$O$_7$; ● = hydroxyapatite; ◆ = CaHPO$_4$·2H$_2$O; □ = γ-Ca$_2$P$_2$O$_7$; ○ = β-Ca$_2$P$_2$O$_7$.

Figure 2. X-ray diffraction patterns of DPG-D heated in a SiC furnace at various temperatures. ◆ = CaHPO$_4$·2H$_2$O; ■ = γ-Ca$_2$P$_2$O$_7$; ● = β-Ca$_2$P$_2$O$_7$; ▲ = α-Ca$_2$P$_2$O$_7$. RT = room temperature.

dentin powder, the X-ray diffraction pattern of the resulting mixture, DPG-D, was identified as dicalcium phosphate dihydrate (CaHPO$_4$·2H$_2$O). The reaction between DPGP and dentin powder produced this compound and caused the peaks representing hydroxyapatite to disappear. The X-ray diffraction pattern of DPG-D after CO$_2$ laser irradiation, shown in Figure 1D, was significantly different from that of DPG-D without irradiation (Figure 1C). The characteristic peaks of DPG-D with CO$_2$ laser irradiation were identified as γ-Ca$_2$P$_2$O$_7$ and β-Ca$_2$P$_2$O$_7$.

Because precisely determining the temperature rise during CO$_2$ laser irradiation and predicting the phase transformation of DPG-D were quite difficult, we heated DPG-D in a SiC furnace to study the phase transformations resulting from an increase in temperature. The DPG-D was heated at various temperatures, and several characteristic peaks belonging to γ-Ca$_2$P$_2$O$_7$ and

β-Ca$_2$P$_2$O$_7$ were identified. While the crystalline phase of DPG-D was CaHPO$_4$·2H$_2$O (Figure 2) at room temperature, when its temperature was raised to 500°C, γ-Ca$_2$P$_2$O$_7$ appeared. At 700°C, the DPG-D transformed to β-Ca$_2$P$_2$O$_7$, which was observable until 1100°C. The α-Ca$_2$P$_2$O$_7$ replaced β-Ca$_2$P$_2$O$_7$ as the major crystalline phase above 1200°C. Thus, it represented that the temperature of DPG-D upon CO$_2$ laser treatment was about 500–1100°C.

DTA/TGA

The DTA results of DPG-D are shown in Figure 3A. The solid line and dotted line represent the DPG-D before and after CO$_2$ laser irradiation, respectively. While these two curves shared a similar pattern, the weaker intensities were found on the dotted line. The DTA curve of DPG-D before CO$_2$ laser irradiation demonstrated a combination of endothermic and exothermic reactions. Two relatively strong endothermic peaks appeared at 82°C and 149°C. The exothermic peaks around
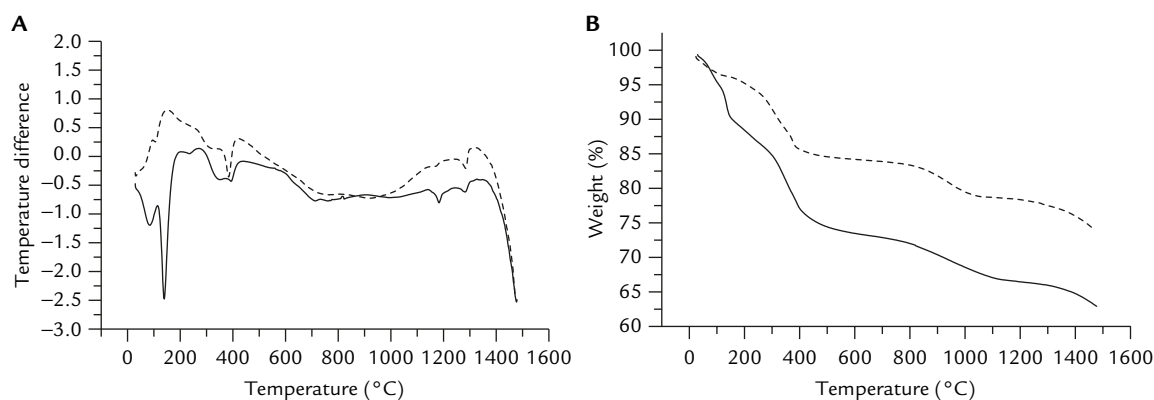
Figure 3. (A) DTA curves and (B) TGA curves of DPG-D. The solid line is before CO_2 laser treatment and the dotted line is after CO_2 laser irradiation.

287°C combined to form a broad curve, which was not as sharp as the curve formed by the endothermic peaks. Three fairly weak endothermic peaks appeared at 347°C, 401°C and 703°C. Another sharp endothermic peak at 1193°C was noted. After CO_2 laser treatment, represented by the dotted line, the endothermic peak at 149°C disappeared and the peak at 82°C became weaker.

Figure 3B shows the results of TGA analysis for DPG-D. Similar to the DTA curves, the solid and dotted lines represent DPG-D before and after CO_2 laser treatment, respectively. These two lines also shared similar patterns with the weaker intensities observable along the dotted line. A significant weight loss of about 25 wt% was recorded for the temperature range between 50°C and 400°C. After 400°C, a moderate weight loss was noted in the TGA curve of DPG-D before CO_2 laser treatment. The total weight loss was about 37.5 wt%. After exposure to the CO_2 laser, the total weight loss was reduced to about 25 wt% as indicated by the dotted line.

Microstructure

Figure 4A shows the longitudinal groove created by a high-speed fissure bur. Figure 4B shows that the gap was sealed by liquid-like melted substance after condensation of DPGP into the groove followed by CO_2 laser irradiation. Figure 4C reveals that the liquid-like melted substance that appeared at Figure 4B was composed of plate-like and globular crystals at higher magnification.

Discussion

The major crystalline phase of DPGP was monocalcium phosphate monohydrate ($Ca(H_2PO_4)_2 \cdot H_2O$) (Figure 1A). Those peaks at the positions of $2\theta = 15.5°$, $32.0°$, $46.1°$ of the DPGP were identified as a second phase, silicate pyrophosphate (SiP_2O_7). When compared to the standard XRD pattern, they corresponded to the crystalline planes of (0 2 0), (0 4 0) and (0 6 0), respectively. The ion exchange and gel formation resulted in paste solidification when the DP-bioactive glass was mixed with phosphoric acid.[17,18] This reaction was suggested as follows:[19]

$$(SiO^-)_2 Ca^{2+} + 2H^+ + 2H_2(PO_4)^- + nH_2O \\ \rightarrow Ca(H_2PO_4)_2 mH_2O + 2Si\text{-}OH \ (m < n) \quad (1)$$
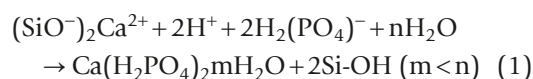
The residual phosphoric acid would further react with Si-OH to form silicate pyrophosphate (SiP_2O_7).
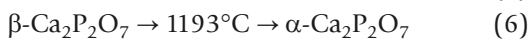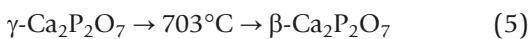
The dentin was composed of nonstoichiometric calcium-deficient hydroxyapatite: $Ca_{10-X}(HPO_4)_X (PO_4)_{6-X}(OH)_{2-X}$ ($0 < X < 2$) which was not well-crystallized compared with stoichiometric hydroxyapatite (Figure 1B).[20] After being mixed with DPGP, dicalcium phosphate dihydrate ($CaHPO_4 \cdot 2H_2O$) was formed (Figure 1C). The proposed reaction was as follows:

$$Ca(H_2PO_4)_2 \cdot H_2O + Ca_5(PO_4)_3(OH) \\ + H_3PO_4 + H_2O \rightarrow 6CaHPO_4 \cdot 2H_2O \quad (2)$$
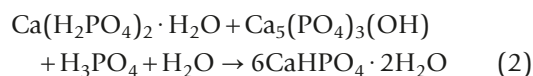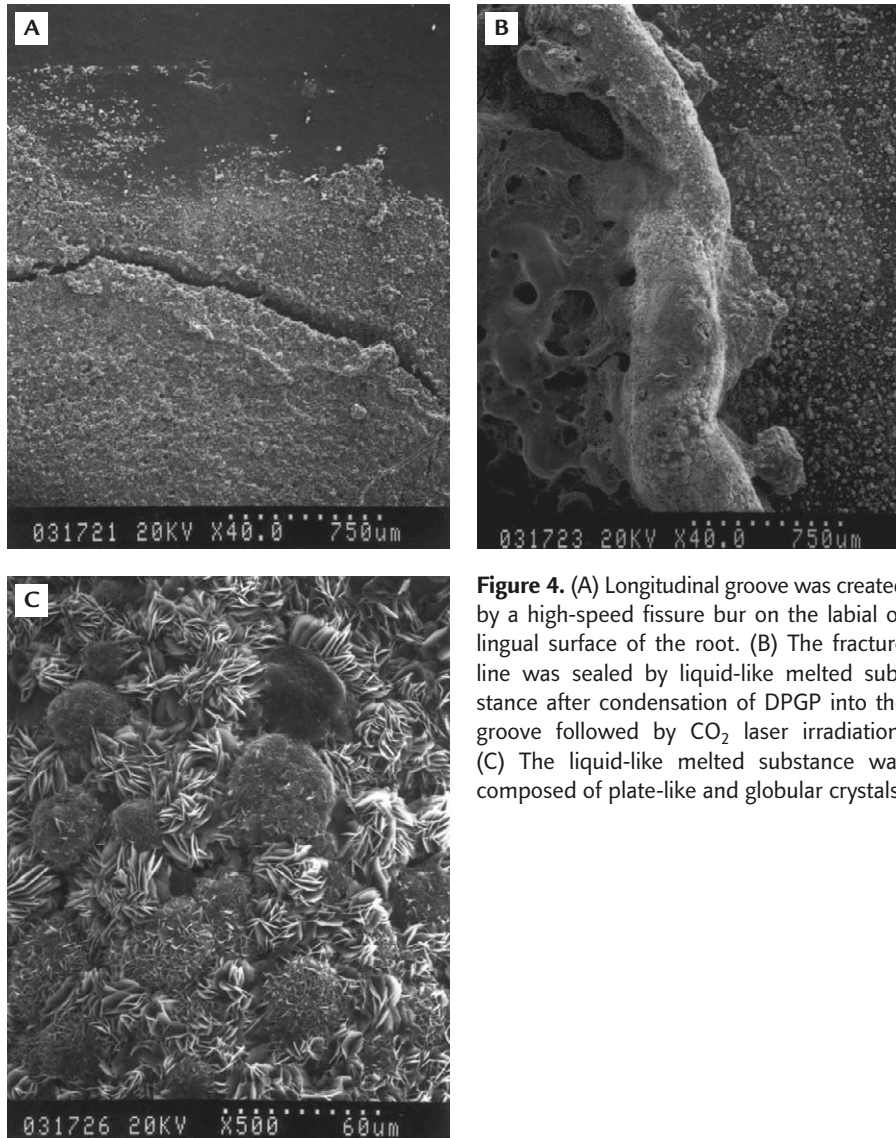
Figure 4. (A) Longitudinal groove was created by a high-speed fissure bur on the labial or lingual surface of the root. (B) The fracture line was sealed by liquid-like melted substance after condensation of DPGP into the groove followed by CO$_2$ laser irradiation. (C) The liquid-like melted substance was composed of plate-like and globular crystals.

From the results of XRD patterns of DPG-D heated at different temperatures (Figure 2), DTA and TGA curves of DPG-D (Figure 3), the phase transformation and chemical reactions are proposed to be as follows:

$$CaHPO_4 \cdot 2H_2O \rightarrow 149°C \rightarrow CaHPO_4 + 2H_2O \quad (3)$$

$$2CaHPO_4 \rightarrow 347°C \rightarrow \gamma\text{-}Ca_2P_2O_7 + H_2O \quad (4)$$

$$\gamma\text{-}Ca_2P_2O_7 \rightarrow 703°C \rightarrow \beta\text{-}Ca_2P_2O_7 \quad (5)$$

$$\beta\text{-}Ca_2P_2O_7 \rightarrow 1193°C \rightarrow \alpha\text{-}Ca_2P_2O_7 \quad (6)$$
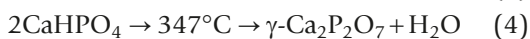
The temperatures mentioned in the above reactions are in agreement with the reports of McIntosh and Jablonski.[21] They stated that the heating of CaHPO$_4$ in the range 325–700°C yielded γ-Ca$_2$P$_2$O$_7$ and β-Ca$_2$P$_2$O$_7$ was formed only over 700°C. The XRD pattern of DPG-D after CO$_2$ laser irradiation demonstrated the appearance of γ-Ca$_2$P$_2$O$_7$ and β-Ca$_2$P$_2$O$_7$ phases (Figure 1D). From the above reactions, the surface temperature induced by CO$_2$ laser might reach as high as 703°C.

DTA of DPG-D before CO$_2$ laser irradiation demonstrated many endothermic peaks and few exothermic reactions (Figure 3A). In the TGA curve of DPG-D before CO$_2$ laser irradiation, water evaporation was the principal reaction with 25% weight loss at 400°C (Figure 3B). The first peak of DTA curve at 82°C was possibly due to surface

water loss. The dicalcium phosphate dihydrate $(CaHPO_4 \cdot 2H_2O)$ further lost water to form $CaHPO_4$ at 149°C. A steep endothermic peak and prominent weight loss could be traced at this temperature. When the temperature was raised to 347°C, the $CaHPO_4$ changed to $\gamma\text{-}Ca_2P_2O_7$. The weight loss was not so significant after 400°C because phase transformation without dehydration was the major reaction. A relatively broad peak at 703°C represented the phase transformation of $\gamma\text{-}Ca_2P_2O_7$ to $\beta\text{-}Ca_2P_2O_7$. The $\beta\text{-}Ca_2P_2O_7$ then changed to $\alpha\text{-}Ca_2P_2O_7$ at 1193°C.

The DTA peaks and TGA curve of DPG-D after laser irradiation was less significant compared with those of DPG-D before laser treatment (Figure 3). After CO_2 laser treatment, the surface water included in the DPG-D was vaporized. Therefore, formation of $\gamma\text{-}Ca_2P_2O_7$ and $\beta\text{-}Ca_2P_2O_7$ instead of drastic water loss in reaction (3) made the peak at 149°C disappear and the peak at 82°C weaker. In addition, the endothermic peaks at temperatures lower than 410°C exhibited relatively lower intensity because the DPG-D was dehydrated by the laser. Moreover, the endothermic peak at 131°C was probably due to the loss of surface absorption water.

According to the study of Ferreira et al,[22] different energy density of CO_2 laser irradiation could cause crazed and cratered enamel with larger apatite crystal size and loss of prismatic structure. The depth of the crazed enamel was about 2–11 μm. In our study, after the DPGP was condensed into a dentin groove and subsequently irradiated by the CO_2 laser, melted masses and plate-like crystals could be observed at the interface (Figure 4). No crazed or cratered dentin was found. We have rationally deduced that the temperature of DPG-D upon CO_2 laser treatment should be between 500°C and 1100°C. The high temperature would produce melted DPG-D. Once the laser irradiation ceased, the outer zone of DPG-D which was in contact with air would result in the formation of many nucleation sites around the interface between DPG-D and air. Consequently, the generation of plate-like crystals took place during the cooling process.[23]

Previous attempts using CO_2 laser alone to treat root fractures have been unsuccessful because the undamaged dentin in proximity to the fracture must be heated to the high melting point of dentin.[11] However, application of the lower melting point of DPGP plus CO_2 laser irradiation could effectively seal the fracture line without damaging the surrounding non-fractured portion of the tooth. Moreover, the lower melting point of DPGP allows the DP-bioglass paste to be melted within seconds after irradiation via a medium energy density continuous-wave CO_2 laser. The high temperature elevation induced by laser irradiation is not a concern because the tooth with root fracture is usually non-vital. Consequently, the results of this study suggest that DPGP in conjunction with a CO_2 laser could be an attractive alternative for treating cases of tooth crack and root fracture. Future *in vivo* studies are advised for more evidence.

Acknowledgments

References

1. Petersen KB. Longitudinal root fracture due to corrosion of an endodontic post. *J Can Dent Assoc* 1971;37:66–8.
2. Tamse A. Iatrogenic vertical root fractures in endodontically treated teeth. *Endod Dent Traumatol* 1988;4:190–6.
3. Wechsler SM, Vogel RI, Fishelberg G, et al. Iatrogenic root fractures: a case report. *J Endodon* 1978;4:251–3.
4. Dang DA, Walton RE. Vertical root fracture and root distortion: effect of spreader design. *J Endodon* 1989;15:294–301.
5. Holcomb JQ, Pitts DL, Nicholls JI. Further investigation of spreader loads required to cause vertical root fracture during lateral condensation. *J Endodon* 1987;13:277–84.
6. Pitts DL, Matheny HE, Nicholls JI. An *in vitro* study of spreader loads required to cause vertical root fracture during lateral condensation. *J Endodon* 1983;9:544–50.
7. Liu J, Kawada E, Oda Y. Effects of surface treatment and joint shape on microtensile bond strength of reattached root dentin segments. *J Prosthet Dent* 2004;91:46–54.

8. Trope M, Rosenberg ES. Multidisciplinary approach to the repair of vertically fractured teeth. *J Endodon* 1992;9:460–3.

9. Schwartz RS, Mauger M, Clement DJ, et al. Mineral trioxide aggregate: a new material for endodontics. *JADA* 1999;130:967–75.

10. Oliet S. Treating vertical root fractures. *J Endodon* 1984; 10:391–6.

11. Dederich DN. CO_2 laser fusion of a vertical root fracture. *JADA* 1999;130:1195–9.

12. Lu HH, Tang A, Oh SC, et al. Compositional effects on the formation of a calcium phosphate layer and the response of osteoblast-like cells on polymer-bioactive glass composites. *Biomaterials* 2005;26:6323–34.

13. Lee BS, Chang CW, Chen WP, et al. *In vitro* study of dentin hypersensitivity treated by Nd:YAP laser and bio-glass. *Dent Mater* 2005;21:511–9.

14. Lee BS, Tsai HY, Tsai YL, et al. *In vitro* study of DP-bioglass paste for treatment of dentin hypersensitivity. *Dent Mater J* 2005;24:562–9.

15. Hench LL. Bioceramic: from concept to clinic. *J Am Ceram Soc* 1991;74:487–510.

16. Regina M, Filgueras T, Torre G, et al. Solution effects on the surface reactions of three bioactive glass compositions. *J Biomed Mater Res* 1993;27:1485–93.

17. Fowler BO. Infrared studies of apatites. II. Preparation of normal and isotopically substituted calcium, strontium, and barium hydroxyapatites and spectra-structure-composition correlations. *Inorg Chem* 1974;13:207–14.

18. Fowler BO, Moreno EC, Brown WE. Infra-red spectra of hydroxyapatite, octacalcium phosphate and pyrolysed octacalcium phosphate. *Arch Oral Biol* 1966;11:477–92.

19. Lin CP, Lin FH, Tseng YC, et al. Treatment of tooth fracture by medium energy CO_2 laser and DP-bioactive glass paste: compositional, structural, and phase changes of DP-bioglass paste after irradiation by CO_2 laser. *Biomaterials* 2000;21:637–43.

20. Lin CP, Lee BS, Lin FH, et al. Phase, compositional, and morphological changes of human dentin after Nd:YAG laser treatment. *J Endodon* 2001;27:389–93.

21. McIntosh AO, Jablonski WL. X-ray diffraction powder patterns of the calcium phosphates. *Analyt Chem* 1956;28: 1424–7.

22. Ferreira JM, Palamara J, Phakey PP, et al. Effects of continuous-wave CO_2 laser on the ultrastructure of human dental enamel. *Archs Oral Biol* 1989;34:551–62.

23. Lee BS, Lin CP, Lin FH, Lan WH. Ultrastructural changes of human dentin after irradiation by Nd:YAG laser. *Lasers Surg Med* 2002;30:246–52.